Materials Physics and Mechanics 17 (2013) 11-16 Received: October 14, 2012

REMARKABLE INFLUENCE OF TERBIUM CATIONS ON THE MAGNETIC PROPERTIES OF COBALT FERRITE NANOPARTICLES

Tahmineh Sodaee[*], Ali Ghasemi[**], Ebrahim Paimozd

Department of Materials Engineering, Malek Ashtar University of Technology, Shahin Shahr, Isfahan, Iran,

*e-mail: t.sodaee@yahoo.com

**e-mail: ali13912001@yahoo.com

Abstract. Terbium substituted cobalt ferrite with composition of $CoFe_{2-x}Tb_xO_4$ nanoparticles (x = 0-0.5) were prepared employing a reverse micelle process. The effect of Tb^{3+} cations substitution on structural and magnetic properties of cobalt ferrite nanoparticles was investigated. X-ray diffraction and field-emission scanning electron microscopy evaluations demonstrated that single phase spinel ferrites with narrow size distribution were obtained. The particle size was beyond the range of superparamagnetic range. Vibrating sample magnetometer was employed to probe the magnetic properties of the samples. It was found that with an increase in terbium content, the coercive field decreases while the saturation of magnetization increases. The Mössbauer spectroscopy was used to determine the site preference of constitutive elements. It is interesting to find that adding terbium cations could enhanced saturation magnetization of cobalt ferrite and make it as a suitable candidate for recording head.

1. Introduction

Cobalt ferrite is a well-known hard magnetic material with a relatively high coercivity, strong magnetocrystalline anisotropy, and moderate saturation of magnetization. Synthesis of nanocrystalline cobalt ferrite has been investigated intensively in recent years for its potential applications in high-density magnetic recording media, microwave devices, and magnetic fluids [1-3]. It has been observed that the magnetic properties of nanocrystalline cobalt ferrite are entirely different from its bulk counterpart, which is not only strongly dependent on particle size, distribution and morphology of crystallites, but also on changes in the cation distribution between the two tetrahedral and octahedral sites [4]. $CoFe_2O_4$ has the inverse spinel structure where Fe^{3+} ions are filled in the tetrahedral and octahedral sites, while Co^{2+} ions are filled in the octahedral sites only. The interesting magnetic properties of ferrimagnetic spinels of the general formula AB_2O_4 originate mainly from the magnetic interactions between cations with magnetic moments that are situated in the tetrahedral and octahedral sites. Certainly, the magnetic interactions will vary with the change of cations in chemical composition and with different cation distribution between the tetrahedral and octahedral sites [5].

Recently, we have focused our studies on the preparation and magnetic characteristics of ferrite nanoparticles [6-10]. Although extensive studies have recently been performed on the fabrication and magnetic characteristics of cobalt ferrite nanoparticles substituted with cations such as Zn^{2+}, Cr^{3+}, La^{3+}, Gd^{3+}, and Nd^{3+} [11-18], to the best of our knowledge no

studies on the terbium (Tb^{3+}) substituted cobalt ferrite have been reported. With this view in mind, current interest is to make terbium substituted cobalt ferrite nanoparticles using reverse micelle technique. Synthesis of various nanoparticles within reverse micelle, specifically ferrites, has demonstrated the ability to control the particle size, size distribution, chemical stoichiometry, and cation occupancy. The structural and magnetic properties of the prepared ferrite nanoparticles were evaluated by employing XRD, FE-SEM, VSM, and MS.

2. Materials and methods

$CoFe_{2-x}Tb_xO_4$ (x = 0-0.5 in a step of 0.1) nanoparticles were prepared by a reverse micelle process. In the preparation of ferrites, two microemulsions with different aqueous phase while water content, w = $[H_2O]/[AOT]$ = 10 kept constant, were synthesized. The first, using a metal solution, and the second one, using ammonium hydroxide. Stock solutions of 0.5 M sodium dioctylsulfosuccinate (AOT) were prepared in isooctane. A metal solution was synthesized using $FeCl_3$, $CoSO_4.7H_2O$, and $Tb(NO_3)_3$ dissolved in water and AOT-isooctane.The second microemulsion was synthesized by mixing ammonia, water, and AOT-isooctane. The second microemulsion was then added to the first one and stirred for 2 h at a room temperature. The pH was adjusted to 10.0 throughout the processing. After rapid magnetic stirring, ethanol was used to extract the surfactant and organic solvent. The colloidal precipitate was sedimented by centrifuging and washed with ethanol and water. The final nanoparticles were heat treated at 400 ˚C for 4 h (In the most of techniques, nanocrystalline cobalt ferrite has been obtained at 1200˚C).

X-ray powder diffraction was performed by employing Cu *kα* radiation. Field-emission scanning electron microscope (FE-SEM) was employed to characterize the morphologies and particle size distribution of the nanoparticles. Vibrating sample magnetometer (VSM) was used to investigate the variation of magnetization with magnetic field. The Mössbauer spectroscopy characterizations were performed in the transmission geometry, using a conventional spectrometer, operated in the constant acceleration mode.

3. Results and discussions

3.1. Structural evaluations. The X-ray diffraction patterns of $CoFe_{2-x}Tb_xO_4$ ferrite nanoparticles with composition of x = 0, 0.3, and 0.5 are presented in Fig. 1. It was found from the patterns that spinel phases can be formed in all the specimens without the existence of any secondary phases. With the gradual increase in rare-earth contents, the materials crystallize with more difficulty. The variation of bond energy will directly lead to the variation of enthalpy [18]. So the increase of bond energy will induce the increase of inner energy, i.e. more energy is needed to form the bond of Tb^{3+}-O^{2-}.

The particle size distribution of the prepared samples were evaluated by using FE-SEM. Figure 2 reflects the FE-SEM micrographs of samples with composition of x = 0, 0.3, and 0.5. The size of nanoparticles is obtained by counting 50 single nanoparticles at various micrographs. It is interesting to find that the terbium cations substitution had no obvious influence on the morphologies, but greatly affected the average crystallite size of the synthesized nanoparticles, that is the average particle size increases with an increase in terbium content. Normally, the rare-earth ions are presented in the grain boundaries; thus the grain growth of cobalt ferrite nanoparticles can be resulted. The control of particle size formed with reverse micelle method is dependent on the size of water pools of microemulsion. The smaller water droplets encapsulated in reverse micelles act as nano-reactors of self-assembled structure, providing an isolated space for the reaction to take place. The size of nano-reactor varies with the water to surfactant molar ratio. These nano-reactors control the size of the nanoparticles and facilitate production of nanoparticles with narrow size distribution [4].

The size distribution obtained for cobalt ferrite nanoparticles by the reverse micelle technique is significantly narrower than that obtained by ball milling, co-precipitation technique, and sol gel process [19-21].

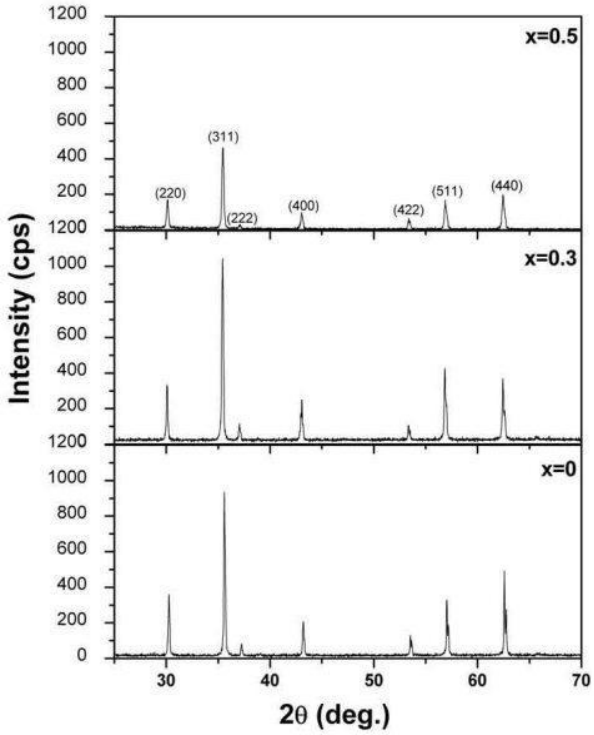

Fig. 1. XRD patterns of $CoFe_{2-x}Tb_xO_4$ ferrite nanoparticles with composition of x = 0, 0.3, and 0.5.

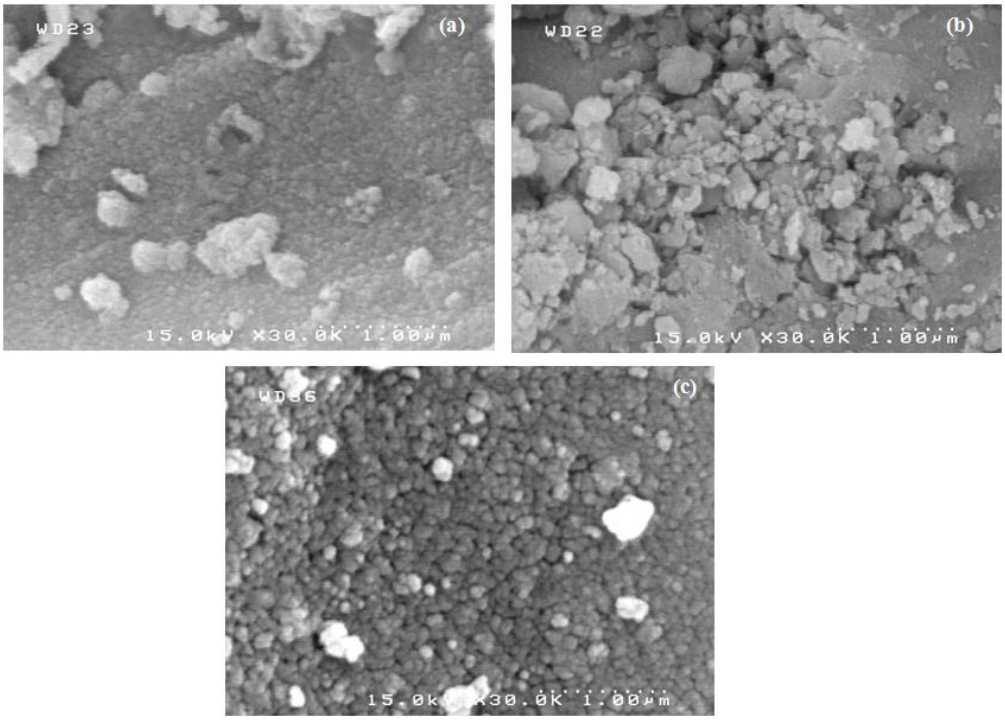

Fig. 2. FE-SEM micrographs of $CoFe_{2-x}Tb_xO_4$ ferrite nanoparticles with composition of (a) x = 0, (b) x= 0.3, and (c) x= 0.5.

3.2. Magnetic properties. Magnetic measurements of samples prepared via reverse micelle, were performed using the VSM technique and the results of magnetic hysteresis at a room temperature are shown in Fig. 3. It was found that with an increase in terbium content, the coercive field decreases. This was expected as coercivity is related to grain size, with larger grains providing less pinning of domain walls because of the lower volume fraction of grain boundaries. Therefore, higher terbium content are expected to result in larger grains and consequently lower coercive field. Interestingly, it has been revealed that terbium cations could inclined the magnetization vector, reduce magnetocrystalline anisotropy of cobalt ferrite, and consequently altered the hard magnetic phase to a soft one. In addition, it is observed from the loop that with increasing terbium content in the composition, the values of saturation magnetization increase. Actually, the variation of saturation magnetization with composition can be estimated by exchange interaction among the cations distributed in the tetrahedral (A) and octahedral (B) sites. It is known that iron ions occupy A and B sites. Terbium cations can be distributed to both sites; however, their preference is in A sites. It must be considered that the magnetic moment of terbium ions is zero at room temperature, while the magnetic moment of iron cations is fixed to be 3 μ_B and 5 μ_B in the A and B sites respectively. With this view in mind, it can be realized that the magnetization of B sublattice is higher than A sublattice. Consequently, the replacement of iron cations situated in tetrahedral sites with terbium cations give a increase in saturation magnetization, which is consistent with our results.

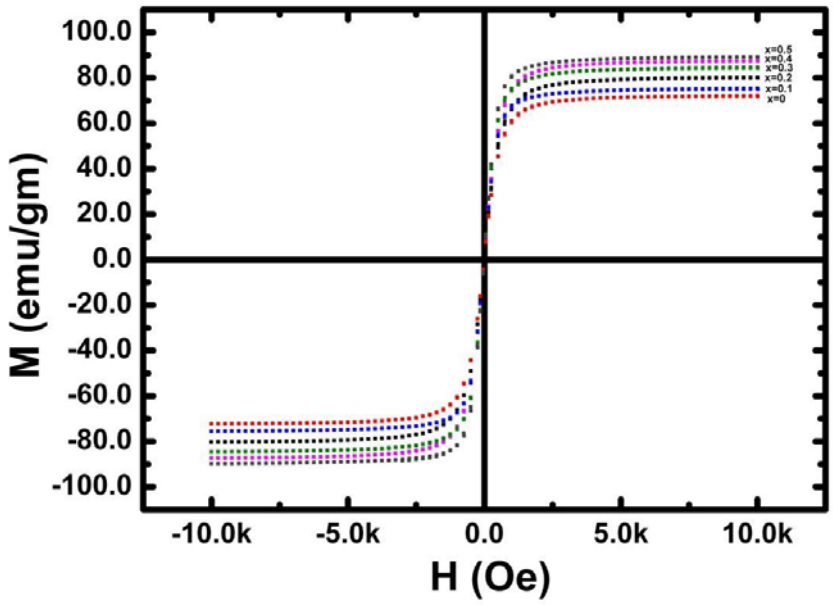

Fig. 3. VSM graphs of $CoFe_{2-x}Tb_xO_4$ ferrite nanoparticles.

The Mössbauer spectroscopy was used to determine the site preference of constitutive elements. Figure 4 shows the Mössbauer spectra of $CoFe_{2-x}Tb_xO_4$ ferrite nanoparticles with composition of x = 0, and 0.5 measured at room temperature. A well-resolved six-line pattern of $CoFe_{2-x}Tb_xO_4$ ferrite nanoparticles is mainly attributed to the ferrimagnetic behavior. It was found that terbium cations were distributed in the tetrahedral and octahedral sites; however, their preference is in tetrahedral sites.

Higher areal densities in magnetic recording media are achieved by using higher-coercivity materials in the media (to stabilize smaller bits), lower head-disk spacing and more sensitive read heads (so that the field lines from the smaller bites can still be detected), and higher-magnetization write heads (to enable writing in the higher coercivity media).

Traditionally recording head were made of cubic ferrites, which are soft, and therefore easily magnetized. However, the saturation magnetizations are not large, so strong magnetic fields cannot be generated. The higher saturation flux density facilitates writing in higher-coercivity media, and allows for narrower track widths and in turn a higher storage density. It is interesting to find that adding terbium cations could enhance saturation magnetization of cobalt ferrite and make it as a suitable candidate for recording head.

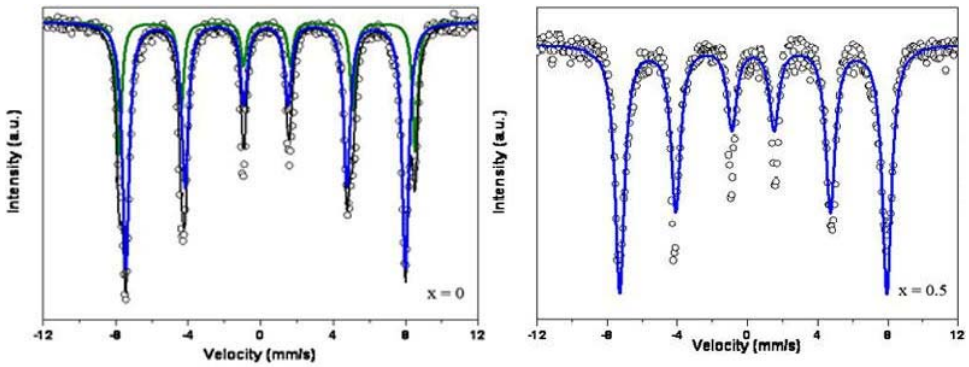

Fig. 4. Mössbauer spectra of $CoFe_{2-x}Tb_xO_4$ ferrite nanoparticles.

4. Conclusions

Fine particles single phase of $CoFe_{2-x}Tb_xO_4$ (x=0-0.5) were prepared by a reverse micelle method. The average particle size increased with an increase in terbium content. It was found that with an increase in terbium amount, the coercive field decreases while the saturation of magnetization increases. The higher saturation of magnetization observed in nanoparticles is attributed to the change in the cation distribution. In addition, the results revealed that terbium cation could reduced magnetocrystalline anisotropy of cobalt ferrite and consequently altered the hard magnetic phase to a soft one.

References

[1] Y. Cedeno-Mattei, O. Perales-Perez // *Microelectronics Journal* **40** (2009) 673.
[2] M. E. Mata-Zamora, H. Montiel, G. Alvarez, J. M. Saniger, R. Zamorano, R. Valenzuele // *Jounal of Magnetism and Magnetic Materials* **316** (2007) e532.
[3] B.E. Kashevsky, V.E. Agabekov, S.B. Kashevsky, K.A. Kekalo, E.Y. Manina, I.V. Prokhorov, V.S. Ulashchik // Particuology **6** (2008) 322.
[4] S. Rana, J. Philip, B. Raj // *Materials Chemistry and Physics* **124** (2010) 264.
[5] M. Han, Ch.R. Vestal, Z.J. Zhang // *J. Phys. Chem. B* **108** (2004) 583.
[6] A. Ghasemi, V. Sepelak, X.X. Liu, A. Morisako // *Journal of Applied Physics* **107** (2010) 09A734.
[7] A. Ghasemi, V. Sepelak, X.X. Liu, A. Morisako // *Journal of Applied Physics* **107** (2010) 09A743.
[8] A. Ghasemi, V. Sepelak, X.X. Liu, A. Morisak // *IEEE Transactions on Magnetics* 45 (2009) 2456.
[9] A. Ghasemi, X.X. Liu, A. Morisako // *IEEE Transactions on Magnetics* **45** (2009) 4420.
[10] A. Ghasemi, A. Morisako // *Journal of Magnetism and Magnetic Materials* **320** (2008) 1167.
[11] J.P. Zhou, Z. Shi, H.C. He, C.W. Nan // *J. Electroceram* **21** (2008) 681.
[12] S.S. Jadhav, S.E. Shirsath, S.M. Patange, K.M. Jadhav // *Journal of Applied Physics* **108** (2010) 093920.

[13] M.H. Yousefi, S. Manouchehri, A. Arab, M. Mozaffari, Gh.R. Amiri, J. Amighian // *Materials Research Bulletin* **45** (2010) 1792.
[14] S.J. Lee, C.C. H. Lo, P.N. Matlage, S.H. Song, Y. Melikhov, J.E. Snyder, D.C. Jiles // *Journal of Applied Physics* **102** (2007) 073910.
[15] P. Kumar, S.K. Sharma, M. Knobel, M. Singh // *Journal of Alloys and Compounds* **508** (2010) 115.
[16] X. Meng, H. Li, J. Chen, L. Mei, K. Wang, X. Li // *Journal of Magnetism and Magnetic Materials* ***321*** (2009) 1155.
[17] J. Peng, M. Hojamberdiev, Y. Xu, B. Cao, J. Wang, H. Wu // *Journal of Magnetism and Magnetic Materials* **323** (2011) 133.
[18] L. Zhao, H. Yang, X. Zhao, L. Yu, Y. Cui, S. Feng // *Materials Letters* **60** (2006) 1.
[19] Y. Qu, H. Yang, N. Yang, Y. Fan, H. Zhu, G. Zou // *Materials Letters* **60** (2006) 3548.
[20] A. Rafferty, T. Prescott, D. Brabazon // *Ceramic International* **34** (2008) 15.
[21] I.H. Gul, A. Maqsood // *Journal of Alloys and Compounds* **465**, (2008) 227.